NANO LETTERS

Letter

pubs.acs.org/NanoLett

Electronic Transport in Porphyrin Supermolecule-Gold Nanoparticle Assemblies

David Conklin,[†] Sanjini Nanayakkara,[†] Tae-Hong Park,[‡,⊥] Marie F. Lagadec,[§] Joshua T. Stecher,[∥] Michael J. Therien,[∥] and Dawn A. Bonnell*[,†]

[†]Department of Materials Science and Engineering and [‡]Department of Chemistry, University of Pennsylvania, Philadelphia, Pennsylvania 19104, United States

[§]Department of Materials, ETH Zurich, Zurich, CH-8093, Switzerland

[∥]Department of Chemistry, French Family Science Center, Duke University, Durham, North Carolina 27708, United States

ABSTRACT: Temperature-dependent transport of hybrid structures consisting of gold nanoparticle arrays functionalized by conjugated organic molecules [(4′-thiophenyl)ethynyl-terminated *meso*-to-*meso* ethyne-bridged (porphinato)zinc(II) complexes] that possess exceptional optical and electronic properties was characterized. Differential conductance analysis distinguished the functional forms of the temperature and voltage dependences for a range of sample particles and molecular attachments. Thermally assisted tunneling describes transport for all cases and the associated mechanistic parameters can be used to determine the relative roles of activation energy, work function, and so forth. These results provide the basis on which to examine plasmon-influenced conduction in hybrid systems.

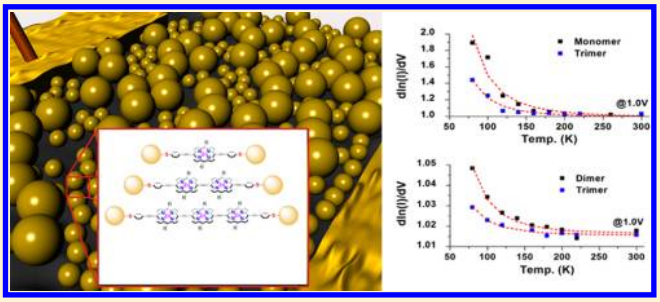

KEYWORDS: *Transport, molecular electronics, porphyrins, nanoparticles*

The electrical properties of molecules have been of interest for decades in the context of molecular electronics, driven in part by the search for post CMOS computation solutions. Experimental approaches to characterizing transport properties have included assembling monolayers on metal surfaces and using planar or tip shaped electrodes or attaching molecules at a break junction of a metallic nanostructures or nanowires.[1−6] In parallel, the understanding of transport in granular media has been evolving.[7] One development here has been the use of molecular linkers to control spacing between metallic nanoparticles in an array.[8] In the case of electronic transport studies, this configuration is analogous to those used in molecular electronics systems, where a substantial number of related results have been reported.

Against this background, we are interested in determining the transport mechanisms relevant to molecule-gold nanoparticle (AuNP) hybrid assemblies that take advantage of *meso*-to-*meso* ethyne-bridged (porphinato)zinc(II) complexes (PZn_n structures). These molecules have been designed to exhibit near "barrierless" transport and global electronic delocalization; congruent with these properties, PZn_n supermolecules feature: (i) high oscillator strength with $S_1 \rightarrow S_n$ and $S_1 \rightarrow S_0$ transitions that extend deep into the near-infrared spectral region, (ii) the largest hole polaron delocalization lengths yet measured for single molecules, and (iii) unusually large polarizabilities.[9−15] Transport in related conjugated multiporphyrin structures has been examined.[16−18] Recently, utilizing α,ω-di[(4′-thiophenyl)-ethynyl]-terminated PZn_n (dithiol-PZn_n) supermolecules, a new mechanism of plasmon-induced current was demonstrated in a system in which these structures are linked to metal nanoparticles.[19,20] Understanding the dark current mechanisms is a prerequisite to exploring the basis of the new transduction phenomenon.[21]

Previous research has shown that alkanethiol monolayers act as insulators; electron transport through such interfaces occurs unambiguously via tunneling.[4,7] For such systems, exponential transport dependences are well documented with barrier heights independent of molecular length.[4,13] In contrast, π-conjugated molecules with molecular orbitals near the electrode Fermi energy mediate electron transport.[22,23] For these molecules, barrier heights are molecular length dependent, resonant tunneling occurs at appropriate energies, and hopping mechanisms are found to contribute in specific cases. However, transport in both insulating and π-conjugated systems is rarely found to be temperature independent, as would be expected for tunneling through a single molecular conformation, even down to 40 K.[4−8,21] Deviations from this expectation would arise from thermally induced changes in the molecule-metal contact geometry or the distribution of molecular configurations. Consequently, transport properties are often described with an empirical relationship that expresses the extent of the

Received: January 30, 2012
Revised: April 5, 2012

dx.doi.org/10.1021/nl300400a | *Nano Lett.* XXXX, XXX, XXX−XXX

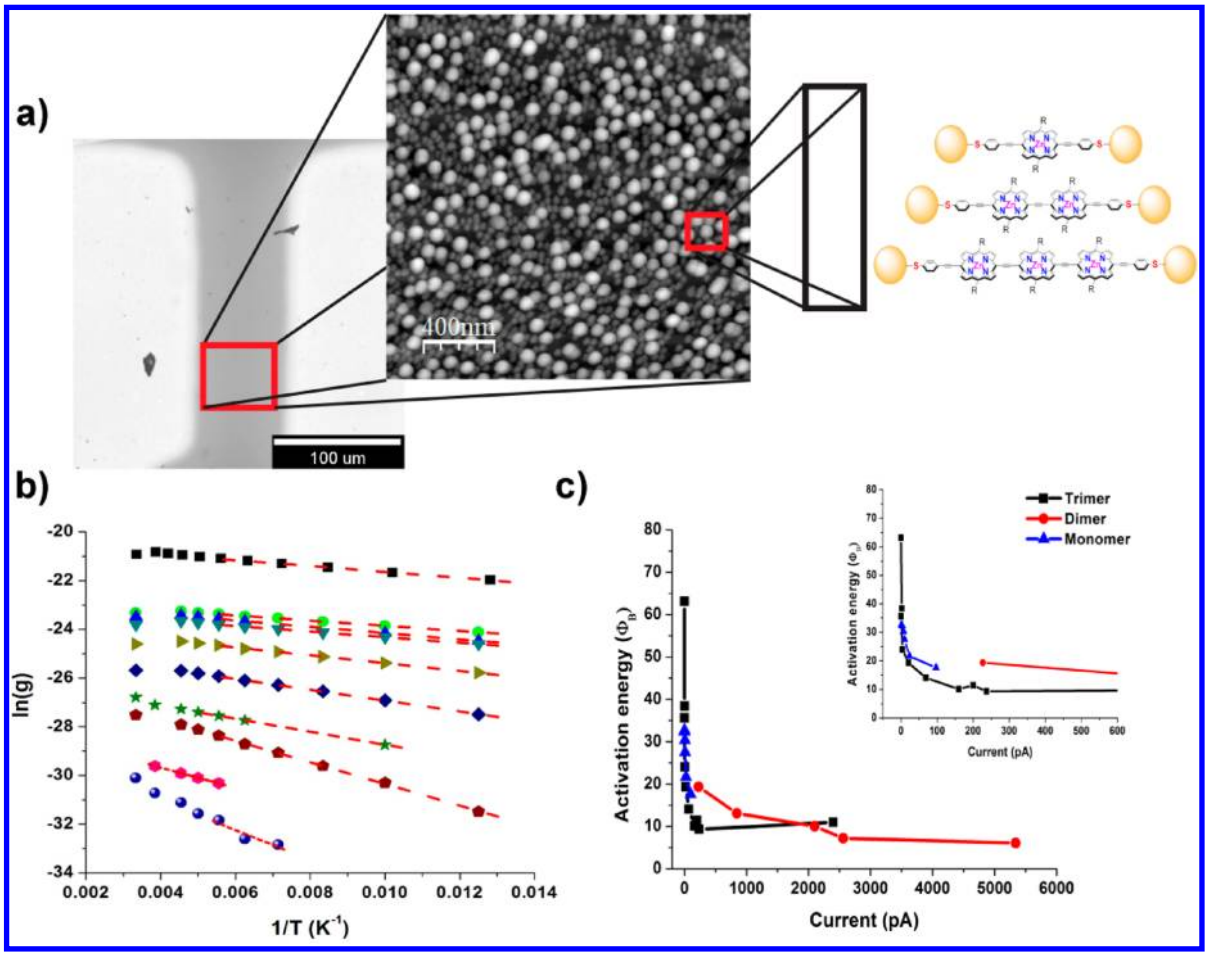

Figure 1. (a) General device configuration in which gold contact pads with a separation of approximately 70 μm were evaporated on top of the AuNP arrays. The expanded region shows an AFM micrograph of the active device area for a bimodal (40 and 15 nm) AuNP array along with a schematic representation of the various dithiol-PZn$_n$ linkers. (b) The inverse temperature dependence as a function of logarithmic conductance of AuNP arrays linked with dithiol-PZn$_3$ supermolecules for samples with various AuNP distributions. (c) The apparent activation energies at 220 K for AuNP arrays linked with dithiol-PZn$_3$ (black), dithiol-PZn$_2$ (red), and dithiol-PZn$_1$ (blue). All samples, regardless of linker molecule or AuNP distribution, exhibit a decrease in activation energy with increasing conductance until it reaches the minimum, approximately 8.6 meV.

attenuation in terms of an exponential decay constant determined from fitting of experimental data (often referred to as the β factor); in related butadiyne-bridged (porphinato)-zinc(II) molecules, β was determined to be on the order of 0.040 Å^{-1}.[16,18] While treatments that utilize empirical temperature-dependent attenuation factors have been effective in comparing the behavior of various transport systems, these are less satisfying with respect to mechanistic clarification.

In this Letter, we examine the transport properties of unique supermolecule/nanoparticle assemblies and take a different approach to the transport analysis, though based on familiar fundamental principles. We experimentally investigate the electronic properties of random arrays of two-dimensional gold nanoparticles (AuNPs) consisting of metal junctions linked by optically active dithiol-PZn$_n$ supermolecules. The conductance of the assemblies was determined as a function of bias voltage, particle size, particle distribution, and the dithiol-PZn$_n$ supermolecule. Using normalized differential conduction analysis, we find that the mechanism is thermally assisted tunneling (TAT), where the response is independent of the particle size and distribution. The nanoparticle arrays were prepared by cleaning glass substrates in piranha solution for 15 min, rinsing with ultrapure milli-Q water, and cleaning in UV ozone for 90 min. The substrates were immediately placed in a nitrogen glovebox and immersed into a 5% solution of 3-aminopropyl-methyl-triethoxysilane (APTES, Sigma-Aldrich) in anhydrous toluene (Sigma-Aldrich) for 60 min. The amine-functionalized glass substrates were then immersed in various citrate-stabilized AuNP solutions (Ted Pella) for 5−220 min. It was found that the immersion time to provide high particle densities was AuNP size dependent with larger particles requiring longer times. The conductivities of the devices were characterized before and after molecular attachment to quantify possible substrate surface conduction and provide a baseline for zero conduction. The syntheses of dithiol-PZn$_n$ structures have been described previously.[19] Adsorption of dithiol-PZn$_n$ onto the AuNP arrays was performed under nitrogen atmosphere. To an acetyl-protected dithiol-PZn$_n$ solution (~1 μM in THF), 4 μL/mL of NH_4OH was added to deprotect the thiolate functionality. The glass substrates with AuNP arrays were then immersed into this solution for 1 h. The substrates were rinsed with THF and dried under nitrogen. Transport measurements were performed using a probe station (Lakeshore Desert Cyrogenics) with an electrometer (Keithley 6515A). The length of the porphyrin-based linker dictates the required interparticle spacing between AuNPs. Nanoparticle morphologies were characterized with atomic force microscopy (Veeco 3100).

dx.doi.org/10.1021/nl300400a | *Nano Lett.* XXXX, XXX, XXX−XXX

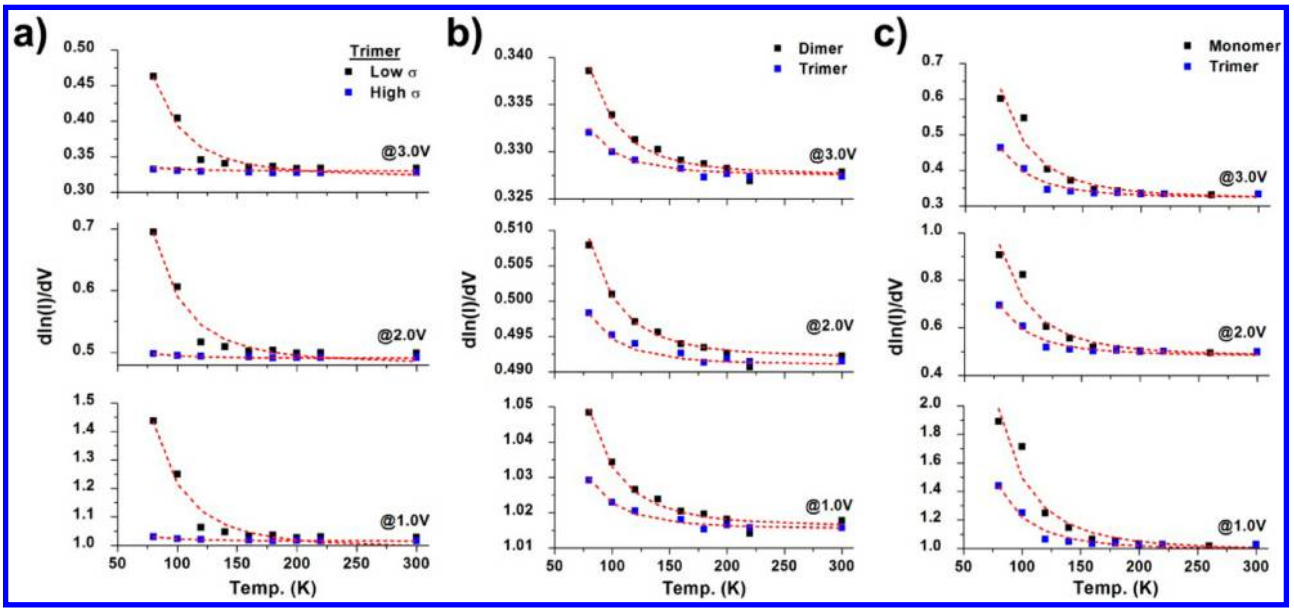

Figure 2. Differential analysis of transport of functionalized AuNPs showing temperature dependence of d ln(I)/dV for a variety of AuNP arrays and supermolecule linkers. (a) Comparison of a low conductivity (40 nm/30 nm bimodal) and high conductivity (40 nm/15 nm bimodal) AuNP arrays linked with dithiol-PZn_3 supermolecules. (b) Comparison of AuNP arrays linked with dithiol-PZn_3 (40 nm/15 nm bimodal) and dithiol-PZn_2 (40 nm/15 nm) supermolecules. (c) Comparison of a AuNP array (40 nm/30 nm bimodal) linked with dithiol-PZn_3 supermolecules with an array (40 nm/15 nm bimodal) linked with dithiol-PZn_1. (b,c) Comparison of AuNP linked arrays of similar conductivity. The dotted lines are the fit of eq 2 with theta as the fitting parameter.

Over 20 devices were analyzed in which nanoparticle arrays varied in diameter (40, 30, 20, and 15 nm), bimodal distribution (40/30 nm, 40/20 nm, and 40/15 nm), and surface coverage (37−83%) (Figure 1). The arrays were linked with a monomeric [5,15-bis[(4′-thiophenyl)ethynyl]-10,20-diarylporphinato]zinc(II) complex (dithiol-PZn_1) and two different α,ω-di[(4′-thiophenyl)ethynyl]-terminated PZn_n supermolecules, a dimer (dithiol-PZn_2), and a trimer (dithiol-PZn_3). Temperature-dependent conductivity measurements were carried out from room temperature to 80 K. The device configuration can be seen in Figure 1a; gold contact pads with a separation of approximately 70 μm were evaporated on top of the masked AuNP arrays; an example of a bimodal array (40 nm/15 nm) of AuNPs is shown in Figure 1a inset. Unlike previous work involving nonconductive alkanethiols adsorbed AuNPs,[7] the conductivity of the porphyrin linked AuNP arrays was found to be only a weak function of AuNP size, distribution and molecular length. The current−voltage responses were near-linear and clear temperature dependence was observed over the entire temperature range.

When the barrier to transport is small, on the order of the size of the linker molecules, tunneling and thermionic (Schottky) emission are generally regarded as the two possible conduction mechanisms. Thermionic emission is strongly dependent on the barrier height and temperature, thus it is easily distinguished from a direct tunneling mechanism. The Poole-Frenkel effect, where the electric field assists thermal ionization of trapped charge carriers, and thermionic emission, where the electric field lowers the barrier height, results in the same functional form of the temperature dependence.[24] Figure 1b compares the temperature dependence of conductance for nine arrays with sizes ranging from 15 to 40 nm and linked with dithiol-PZn_3. Temperature dependence is often interpreted in terms of Arrhenius or hopping models but this analysis requires a priori assumptions of the details of the model. The data in Figure 1b can be fit reasonably well to an Arrhenius model (T^{-1} dependence), or a variable-range hopping model ($T^{-1/2}$ dependence). This does not provide a definitive mechanistic description since the hopping model exponent is often varied to describe site disorder and hence fit a range of properties and it is not clear what energy is determined in the Arrhenius analysis (as discussed below). However, there is more information inherent in the data that we analyze after considering the implications of the "apparent" activation energy.

Figure 1c compares the apparent activation energies obtained from an Arrhenius analysis of AuNP arrays linked with dithiol-PZn_n supermolecules and differing with respect to overall conductance. The two factors that can affect the conductance are the number of pathways of connected nanoparticles and the degree of molecular coverage on the metal surface. The former does not affect the activation energy, but the latter does in that the barrier height is a function of AuNP work function, which is modulated by dithiol-PZn_n adsorption coverage. Adsorption in general decreases the work function of a metal surface and this is specifically shown to be true for thiol on gold surfaces.[25,26] Note also that the three dithiol-PZn_n structures have the same thiol bond to the gold and apparent activation energies approach the same minimal value of 8.6 meV at 220 K, as expected since the thiol-gold bond is the dominant determinant of barrier height. This is convincingly shown for the current versus activation energy data displayed for devices that exploit dithiol-PZn_1 and dithiol-PZn_3 linkers (Figure 1c), and while the data is not as extensive for devices that exploit the dithiol-PZn_2 linker, the trend is consistent. In our case, increased dithiol-PZn_n porphyrin coverage would lower the work function and increase the overall conductance and furthermore, and converge at complete surface coverage. For this reason, the variation in the activation energy was attributed to the extent of the surface coverage of the molecule on the AuNPs, and all analyses of mechanism were carried out on samples with similar

dx.doi.org/10.1021/nl300400a | Nano Lett. XXXX, XXX, XXX−XXX

Table 1. Functional and Differential Forms of Electronic Transport Mechanisms

Fowler-Nordheim tunneling (FN)	$I = A_{\text{eff}}\frac{e^3 m}{8\pi h m \phi_B}E^2 \exp\left(-\frac{8\pi\sqrt{2m}}{3he}\frac{\phi_B^{3/2}}{E}\right)$	$\frac{\mathrm{d}\ln I}{\mathrm{d}V} = \frac{1}{V} + \frac{4\pi}{3he}\sqrt{2m}\frac{\phi_B^{3/2}}{(V)^2}$
thermionic emission (TE)	$I = A_{\text{eff}}A^{**}T^2 \exp\left(-\frac{e}{kT}\left(\phi_B - \sqrt{\frac{eE}{4\pi\varepsilon_0\varepsilon}}\right)\right)$	$\frac{d\ln I}{dV} = \frac{e}{4kT}\left(\frac{e}{\pi\varepsilon_0\varepsilon}\right)^{1/2}(V)^{-1/2}$
Arrhenius type behavior	$I = e\mu n E \exp\left(-\frac{E_f}{kT}\right)$	$\frac{d\ln I}{dE} = E^{-1}$
Poole-Frenkel hopping	$I = e\mu n E \exp\left(-\frac{e}{kT}\left(E_i^0 - \sqrt{\frac{eF}{4\pi\varepsilon_0\varepsilon}}\right)\right)$	$\frac{d\ln I}{dE} = \frac{1}{E} + \frac{1}{kT}\sqrt{\frac{e^3}{4\pi\varepsilon_0\varepsilon}}E^{-0.5}$
thermally assisted tunneling (TAT)	$I = \frac{E}{2\pi}\left(\frac{kTt}{2\pi}\right)^{1/2}\exp\left(-\frac{\phi}{kT} + \frac{E^2\Theta}{24(kT)^3}\right)$	$\frac{d\ln I}{dV} = V^{-1} + \left(\frac{V\Theta}{12(kT)^3}\right)$

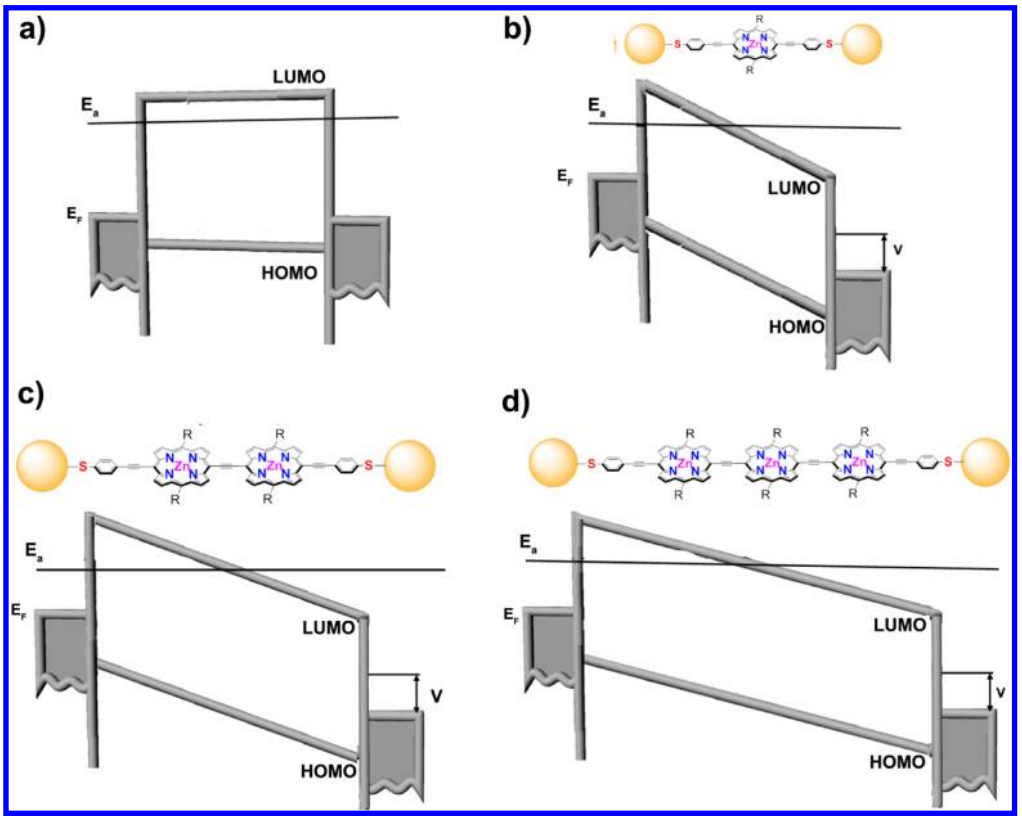

Figure 3. Idealized band diagram for AuNP arrays linked with dithiol-PZn$_n$ structures of varying length. (a) The flat band condition, where E_F is the Fermi energy of the AuNPs in relation to the HOMO−LUMO levels of the dithiol-PZn$_n$ supermolecules. E_a is the energy at some level above the Fermi level in which thermally assisted tunneling occurs. (b−d) The cases for dithiol-PZn$_1$, dithiol-PZn$_2$, and dithiol-PZn$_3$, respectively, with an applied voltage across the junction.

conductivities, ensuring that the work functions were likewise similar. The ambiguity in the mechanism from a priori analyses of the temperature dependence can be addressed by employing current-normalized differential conductance, which allows the temperature dependence, the field dependence, and the temperature dependence of the field dependence to be examined.[27] With these interdependencies, complex transport mechanisms may be distinguishable.

Figure 2 shows the transport properties for arrays linked to dithiol-PZn$_1$ and supermolecules dithiol-PZn$_2$ and dithiol-PZn$_3$. For each type of dithiol-PZn$_n$-linked array, two examples are compared: one with higher overall network conductance and one with lower conductance. As noted above, this enables comparison of high molecular coverage (higher conductance) and lower coverage (lower conductance). We performed analysis of transport of functionalized AuNP arrays by fitting possible transport mechanisms (Table 1). For example, inspection of the functional form from current-normalized differential conductance of a thermionic emission or Poole-Frenkel model reveals an inverse temperature dependence. However, differential analysis of the temperature dependence for high and low conductance (Figure 2a), and comparisons of dithiol-PZn$_3$ linked arrays with dithiol-PZn$_2$ (Figure 2b) and dithiol-PZn$_1$ linked (Figures 2c) arrays demonstrate that the thermionic emission model does not fit to the behaviors of PZn$_n$-Au NP arrays. Similar analysis for other possible mechanisms, led us to propose that thermally assisted tunneling is the mechanism controlling transport.

dx.doi.org/10.1021/nl300400a | Nano Lett. XXXX, XXX, XXX−XXX

The early foundational papers by Murphy and Good and Roberts and Polanco provide a framework within which to consider the possibility of multiple transport paths.[28,29] They considered a continuous range of transport behaviors between direct tunneling as one limiting case and thermionic emission as the other. Furthermore, Roberts describes thermally assisted tunneling as the case where the major contribution to the tunneling integral does not arise from the Fermi level, but from an energy level above the Fermi level. If thermally assisted tunneling contributes significantly to transport, the measured apparent barrier heights are smaller than the expected barrier to transport since this contribution comes from the energies that are above the Fermi energy. This is analogous to a nonideal Schottky barrier. In cases between the two limits, transport consists of both thermionic and tunneling or field emission and is represented by the functional form in eq 1, where I is the current, V is the applied voltage, T is the temperature, k is the Boltzmann constant, $t(y)$ is an elliptical function, and Θ is a function of both elliptic functions $v(y)$ and $t(y)$.

$$I = \frac{V}{2\pi}\left(\frac{kTt(y)}{2\pi}\right)^{1/2} \exp\left(-\frac{\phi}{kT} + \frac{V^2\Theta}{24(kT)^3}\right) \quad (1)$$

$$\frac{d\ln I}{dV} = V^{-1} + \left(\frac{V\Theta}{12(kT)^3}\right) \quad (2)$$

The fit curves (red dotted lines) in Figure 2 show that in all cases the functional form of eq 2 is in excellent agreement with the measurements. This is true regardless of the nanoparticle distribution, the molecular linker, and the conductance. In contrast, for both the Fowler-Nordheim and Arrhenius cases, the differential analysis results in no temperature dependence, while thermionic emission and Poole-Frenkel hopping result in inverse temperature dependences. Thermally assisted tunneling exhibits a vastly different cubic temperature dependence, which easily distinguishes it from both the thermionic emission and Poole-Frenkel mechanisms.

The work function of the nanoparticles with chemisorbed dithiol-PZn$_n$ linkers is not known but comparison of Θ and the Arrhenius behavior provides useful insight. As noted above, Θ is associated with thermally assisted tunneling and is a function of applied field and the barrier height.[30] The fit of eq 2, shown in Figure 2 yields $\Theta = 1.34 \times 10^{-8} - 3.69 \times 10^{-7}$, for the range of arrays tested. These values correspond to the situation where the number of active junctions in the array is small and barrier heights are similar in magnitude to those obtained from Arrhenius analysis (10−30 meV). The Θ determined from the measurements increases as a function of dithiol-PZn$_n$ molecular length, which can be understood as a decrease in the local electric field due to the increased particle separation. Similarly an observed increase in Θ as a function of decreasing conductivity is consistent with a decrease in the apparent barrier height expected for higher molecular surface coverage on the AuNPs. So not only does this approach identify the transport mechanism, it provides parameters associated with local properties.

This transport process is illustrated in Figure 3, which shows an idealized band diagram as a function of molecular length. For a given applied bias and equal number of junctions, the increased molecular length implies a lower local electric field. At temperatures above 0 K, there is a distribution of electrons above the Fermi energy (not shown in the schematic diagram). The energy at which the majority of tunneling occurs is above the Fermi energy (at temperatures above 0 K) but below the LUMO and, therefore, likely associated with an energetic metal or molecular state, as expected for a thermally assisted tunneling mechanism. Interestingly, Sedghi et al. come to a similar conclusion regarding the mechanism of charge transport mediated by *meso*-to-*meso* butadiyne-bridged (porphinato)zinc(II) structures by comparing single molecule measurements with calculations of transmission coefficients.[16] They associate increased temperature dependence with the alignment of the Fermi level and molecular orbitals.

In summary, we report the conductance properties of two-dimensional arrays of AuNP linked by various length optically active α,ω-di[(4′-thiophenyl)ethynyl]-terminated *meso*-to-*meso* ethyne bridged (porphinato)zinc(II) structures (dithiol-PZn$_n$ supermolecules). Differential conductance analysis distinguished the functional forms of the temperature and voltage dependences for a range of sample configurations and molecular attachments. The conduction is attributed to thermally assisted tunneling, with the variation from 8−45 meV in apparent activation energy assigned to variations in the AuNP molecular coverage, while variation in conductivity derives from the modulation of the electric field across the junction as a function of molecular length. The theta parameter in the thermally assisted tunneling model allows for the comparison of the role of structure and properties in similar transport systems. These results provide the basis on which to examine plasmon-influenced conduction in hybrid systems.

AUTHOR INFORMATION

Corresponding Author

*E-mail: bonnell@seas.upenn.edu

Present Address

⊥Nuclear Chemistry Research Division, Korea Atomic Energy Research Institute (KAERI), Daejeon, 305-353, Korea.

Notes

The authors declare no competing financial interest.

ACKNOWLEDGMENTS

Support from the NanoBio Interface Center (NBIC) NSF NSEC DMR04-25780 is acknowledged, as is support of the NBIC facilities. M.J.T. is grateful to the Division of Chemical Sciences, Geosciences, and Biosciences, Office of Basic Energy Sciences of the U.S. Department of Energy through Grant DE-SC0001517 for funding the development of these electro-optically functional porphyrin-based supermolecules. We benefitted from valuable discussion with Peter Maksymovych.

REFERENCES

(1) Heath, J. R.; Ratner, M. A. *Phys. Today* **2003**, *56*, 43−49.
(2) Scott, J. C. *J. Vac. Sci. Technol., A* **2003**, *21*, 521−531.
(3) Kushmerick, J. G.; Holt, D. B.; Pollack, S. K.; Ratner, M. A.; Yang, J. C.; Schull, T. L.; Naciri, J.; Moore, M. H.; Shashidhar, R. *J. Am. Chem. Soc.* **2002**, *124*, 10654−5.
(4) Wang, W.; Lee, T.; Reed, M. A. *Phys. Rev. B* **2003**, *68*, 035416.
(5) Selzer, Y.; Cabassi, M. A.; Mayer, T. S.; Allara, D. L. *J. Am. Chem. Soc.* **2004**, *126*, 4052−4053.
(6) Xing, Y. J.; Park, T. H.; Venkatramani, R; Keinan, S; Beratan, D. N.; Therien, M. J.; Borguet, E. *J. Am. Chem. Soc.* **2010**, *132*, 7946−7956.
(7) Zabet-Khosousi, A.; Dhirani, A. A. *Chem. Rev.* **2008**, *108*, 4072−4124.
(8) Schmid, G.; Simon, U. *Chem. Commun.* **2005**, 697−710.

(9) Susumu, K.; Therien, M. J. *J. Am. Chem. Soc.* **2002**, *124*, 8550−8552.
(10) Shediac, R.; Gray, M. H. B.; Uyeda, H. T.; Johnson, R. C.; Hupp, J. T.; Angiolillo, P. J.; Therien, M. J. *J. Am. Chem. Soc.* **2000**, *122*, 7017−7033.
(11) Lin, V. S. Y.; DiMagno, S. G.; Therien, M. J. *Science* **1994**, *264*, 1105−1111.
(12) Lin, V. S. Y.; Therien, M. J. *Chem.—Eur. J.* **1995**, *1*, 645−651.
(13) Rubtsov, I. V.; Susumu, K.; Rubtsov, G. I.; Therien, M. J. *J. Am. Chem. Soc.* **2003**, *125*, 2687−2696.
(14) Duncan, T. V.; Susumu, K.; Sinks, L. E.; Therien, M. J. *J. Am. Chem. Soc.* **2006**, *128*, 9000−9001.
(15) Susumu, K.; Frail, P. R.; Angiolillo, P. J.; Therien, M. J. *J. Am. Chem. Soc.* **2006**, *128*, 8380−8381.
(16) Sedghi, G.; Sawada, K.; Esdaile, L. J.; Hoffmann, M.; Anderson, H. L.; Bethell, D.; Haiss, W.; Higgins, S. J.; Nichols, R. J. *J. Am. Chem. Soc.* **2008**, *130*, 8582−+.
(17) Kang, B. K.; Aratani, N.; Lim, J. K.; Kim, D.; Osuka, A.; Yoo, K. H. *Chem. Phys. Lett.* **2005**, *412*, 303−306.
(18) Sedghi, G.; Garcia-Suarez, V. M.; Esdaile, L. J.; Anderson, H. L.; Lambert, C. J.; Martin, S.; Bethell, D.; Higgins, S. J.; Elliott, M.; Bennett, N.; Macdonald, J. E.; Nichols, R. J. *Nat. Nanotechnol.* **2011**, *6*, 517−523.
(19) Banerjee, P.; Conklin, D.; Nanayakkara, S.; Park, T.-H.; Therien, M. J.; Bonnell, D. A. *ACS Nano* **2010**, *4*, 1019−1025.
(20) Conklin, D.; Park, T.-H.; Nanayakkara, S.; Therien, M. J.; Bonnell, D. A. *Adv. Funct. Mater.* **2011**, *21*, 4598−4598.
(21) Frisbie, C. D.; Choi, S. H.; Kim, B. *Science* **2008**, *320*, 1482−1486.
(22) Beebe, J. M.; Kim, B.; Frisbie, C. D.; Kushmerick, J. G. *ACS Nano* **2008**, *2*, 827−32.
(23) Zangmeister, C. D.; Robey, S. W.; van Zee, R. D.; Yao, Y.; Tour, J. M. *J. Phys. Chem. B* **2004**, *108*, 16187−16193.
(24) Sze, S. M.; Ng, K. K. *Physics of semiconductor devices*, 3rd ed.; Wiley-Interscience: Hoboken, NJ, 2007.
(25) Zhou, J.; Acharya, D.; Camillone, N.; Sutter, P.; White, M. G. *J. Phys. Chem. C* **2011**, *115*, 21151−21160.
(26) Malicki, M.; Guan, Z.; Ha, S. D.; Heimel, G.; Barlow, S.; Rumi, M.; Kahn, A.; Marder, S. R. *Langmuir* **2009**, *25*, 7967−7975.
(27) Maksymovych, P.; Pan, M. H.; Yu, P.; Ramesh, R.; Baddorf, A. P.; Kalinin, S. V. *Nanotechnology* **2011**, 22.
(28) Murphy, E. L.; Good, R. H. *Phys. Rev.* **1956**, *102*, 1464−1473.
(29) Polanco, J. I.; Roberts, G. G. *Phys. Status Solidi A* **1972**, *13*, 603−&.
(30) The term Θ is a function of v and t, which are mathematical definitions that depend only on the Nordheim parameter y. $\Theta = 3/t^2 - 2v/t^3$ and $y = cF^{1/2}/h$ where F is the barrier field, c is a constant, and h is the barrier height. Fitting the differential conductance with eq 2 using theta as a fitting parameters when the work function is known yields the local electric field. If the work function is not known, the limits of the field dependence can be determined from the limits of the expected work function values.